Hand-powered ultralow-cost paper centrifuge

M. Saad Bhamla[1], Brandon Benson[1†], Chew Chai[1†], Georgios Katsikis[2], Aanchal Johri[1] and Manu Prakash[1*]

In a global-health context, commercial centrifuges are expensive, bulky and electricity-powered, and thus constitute a critical bottleneck in the development of decentralized, battery-free point-of-care diagnostic devices. Here, we report an ultralow-cost (20 cents), lightweight (2 g), human-powered paper centrifuge (which we name 'paperfuge') designed on the basis of a theoretical model inspired by the fundamental mechanics of an ancient whirligig (or buzzer toy; 3,300 BC). The paperfuge achieves speeds of 125,000 r.p.m. (and equivalent centrifugal forces of 30,000 g), with theoretical limits predicting 1,000,000 r.p.m. We demonstrate that the paperfuge can separate pure plasma from whole blood in less than 1.5 min, and isolate malaria parasites in 15 min. We also show that paperfuge-like centrifugal microfluidic devices can be made of polydimethylsiloxane, plastic and 3D-printed polymeric materials. Ultracheap, power-free centrifuges should open up opportunities for point-of-care diagnostics in resource-poor settings and for applications in science education and field ecology.

A centrifuge is the workhorse of any medical diagnostics facility. From the extraction of plasma from whole blood (for performing immunoassays or determining the haematocrit value), to analysing the concentration of pathogens and parasites in biological fluids, such as blood, urine and stool (for microscopy), centrifugation is the first key-step for most diagnostic assays[1]. In modern diagnostics, separation of unwanted cellular debris is especially critical for the accuracy and reliability of molecular diagnostics tools and lateral-flow-based rapid diagnostic tests[2] that are designed for detecting low levels of infection in diseases such as malaria, human immunodeficiency virus and tuberculosis[3–5]. Currently, centrifugation is typically inaccessible under field conditions, because conventional machines are bulky, expensive and electricity-powered[4]. The need for electricity-free centrifugal bio-separation solutions has prompted researchers to use egg-beaters and salad-spinners as proposed devices[6,7]. However, these suffer from bulky designs and extremely low rotational speeds (maximum 1,200 r.p.m.; 300 g), leading to impractical centrifugation times for a simple task of blood plasma separation (>10 min). Thus, a low-cost, portable, human-powered centrifuge that achieves high speeds is an essential, yet unmet need, especially for diagnostics in resource-limited environments[8–10].

We describe the design and implementation of an ultralow-cost (<20 cents, Supplementary Table 5), lightweight (2 g), field-portable centrifuge, henceforth referred to as a 'paperfuge' and inspired by historic whirligig (or buzzer) toys (Fig. 1a). We demonstrate that the paperfuge achieves speeds of 125,000 r.p.m. (30,000 g) using only human power. Using a combination of modelling and experimental validation, we uncover the detailed mechanics of the paperfuge and leverage this understanding to construct centrifuges from different materials (in particular, paper and plastic). We demonstrate applications including plasma separation, quantitative buffy coat analysis (QBC) and integrated centrifugal microfluidic devices for point-of-care (POC) diagnostic testing.

Supercoiling-mediated ultrafast spinning dynamics

We started by measuring the speed of a whirligig (circular discs spun by pulling on strings passing through their centre; Fig. 1a and Supplementary Fig. 1) made out of a paper disc or paperfuge (Fig. 1b; radius of the central paper disc, $R_d = 50$ mm), using a high-speed camera with a fast video-recording frame-rate, ($f_{rec} = 6,000$ frames

per second (f.p.s.); Fig. 1c, Supplementary Fig. 3 and Supplementary Videos 1 and 2). The actuation of the paperfuge consists of successive 'unwinding' and 'winding' phases (Fig. 1d). In the unwinding phase, the outward input force (applied by human hands on the handles) accelerates the disc to a maximum rotational speed ($\dot{\phi}_{max}$). In the winding phase, the input force falls to zero, allowing the inertia of the disc to rewind the strings and draw the hands back inwards. Since the strings are flexible (low bending stiffness), they wind beyond the geometric zero-twist point[11], passing through a spectrum of helical twisting states. After reaching a tightly packed supercoiled state[12,13] (Fig. 1c, insets), the motion of the disc comes to a momentary halt. At this point, an outward force is re-applied, unwinding and winding the strings. This cycle repeats itself at a frequency f_0. Figure 1e shows the maximum rotation speeds of paperfuge devices with radii ranging from 5 to 85 mm. We find that the radius of the central disc strongly influences the maximum speed achieved. The smallest disc ($R_d = 5$ mm) reached a $\dot{\phi}_{max}$ of 125,000 r.p.m. at $f_0 = 2.2$ Hz (Fig. 1e). It is worth noting that muscle force–velocity tradeoff constrains the fastest operable frequency[14] at 2 Hz. To the best of our knowledge, 125,000 r.p.m. is the fastest rotational speed reported via a human-powered device. We have submitted an application to Guinness World Records.

By optimizing the buzzer for high-speed operation and driving it using human hands, we achieved roughly two orders of magnitude faster rotation speeds than previously reported[15]. Motivated by this experimental finding, we developed a detailed theoretical model that faithfully captures the extensive parameter space of this system.

Paperfuge as a nonlinear oscillator

We describe the buzzer toy as a nonlinear, non-conservative oscillator: in every rotation cycle, the input energy is introduced by human hands (applied force) and is dissipated by the system through air drag and in the strings. We consider a massless, inextensible string with uniform tension throughout the string (Fig. 2a). Starting from an energy balance on the system (Supplementary Information), we derived a governing equation of motion that relates angular acceleration $\ddot{\phi}$ and different torque components as:

$$I\ddot{\phi} = \tau_{Input}(\phi) + \tau_{Drag}(\dot{\phi}) + \tau_{Twist}(\phi) \qquad (1)$$

[1]Department of Bioengineering, Stanford University, Stanford, California 94305, USA. [2]Department of Mechanical Engineering, Stanford University, Stanford, California 94305, USA. [†]These authors contributed equally to this work. *e-mail: manup@stanford.edu
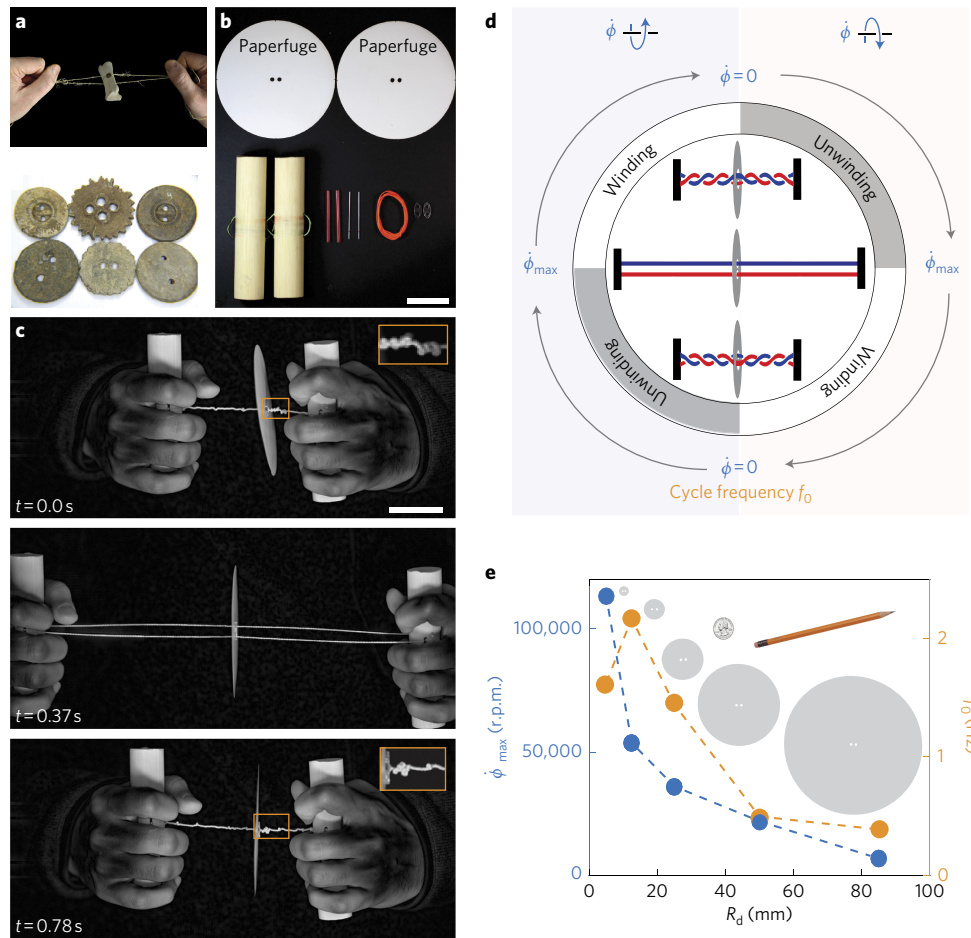
Figure 1 | Spinning dynamics of a paperfuge. a, Top: whirligig (or buzzer toys): image of an ancient buzz bone tied to a raw-hide, used as a charm to ward off evil spirits (reproduced with permission from the University of Cambridge Museum of Archaeology and Anthropology). Bottom: lead whirligig relics with saw-tooth edges (reproduced with permission from R. Dee and J. Winter, http://www.johnwinter.net/jw/2014/07/the-lead-whirligig). **b**, Materials used to construct the paperfuge include two paper discs, wooden handles, string, capillaries, capillary holders and plastic shims (see Methods). **c**, Images of a rotating paperfuge captured with a high-speed camera ($f_{rec} = 6{,}000$ f.p.s.) and showing a succession of wound (top), unwound (middle) and re-wound (bottom) states, for half a cycle. The entire process pictured occurred within a second (Supplementary Video 1). The insets show the supercoiling of the strings during the wound states. Scale bars in **b** and **c** are 5 cm. **d**, Schematic illustrating the periodic rotation of the paperfuge where the disc starts at zero rotational speed ($\dot{\phi} = 0$) and then cycles to $\dot{\phi}_{max}$. **e**, Plot of $\dot{\phi}_{max}$ and f_0 for different hand-powered discs (with R_d of 5, 12.5, 25, 50 and 85 mm, Supplementary Table 3). Scaled images of the disc sizes in relation to a US quarter and a pencil are included for visual comparison.

where I is the inertial moment of the disc, ϕ is the angular displacement, and τ_{Input}, τ_{Drag} and τ_{Twist} are the ϕ, air-drag and string-twisting contributions to the torque, respectively. Each of the above terms can be derived from the geometrical parameters of the system (Supplementary Information).

We first started with the input torque that is dependent on the applied pull force as $\tau_{Input}(\phi) = -\,\text{sgn}(\phi) 2 R_s F \tan\theta$, where R_s is the radius of the string, F is the force applied by hand and θ is the angle subtended by the string from the axial axis of the paper disc. To evaluate $\tau_{Input}(\phi)$, we had to find the relationship between θ and ϕ. We divided the twisting section of the string into three parts (l_1, l_2 and l_3; Supplementary Figs 4 and 5) and obtained a geometrical relationship between θ and ϕ, where $\theta = \sin^{-1}(|\phi| R_s + R_h + R_w) / L)$, R_h the handle radius, $2R_w$ the distance between the holes on the disc, and $4L$ the total length of the string. This gives the formulation:

$$\tau_{Input} = -\,\text{sgn}(\phi) 2 R_s F \frac{|\phi| R_s + R_h + R_w}{\sqrt{L^2 - (|\phi| R_s + R_h + R_w)^2}} \quad (2)$$

Since the Reynolds number for the spinning disc is large ($\text{Re} \approx 10^5$), we calculated the component due to air drag as $F_{Drag}(\dot{\phi}) = -\,a_R S_d (R_d \dot{\phi})^2$, where a_R is the air-friction parameter, and S_d is the surface element on the disc. Integrating over the total surface area of a paper disc of width w, we obtained the following expression for the drag torque:

$$\tau_{Drag}(\dot{\phi}) = -\,\text{sgn}(\dot{\phi}) a_R \left(\frac{4\pi}{5} R_d^5 + 2\pi w R_d^4 \right) \dot{\phi}^2 \quad (3)$$

The twisting term (τ_{Twist}) accounts for many forces in the paperfuge dynamics that contribute to the string's resistance to twisting. Since the strings have low stiffness in both bending and torsion, they undergo twist far beyond the zero-twist point (Supplementary Fig. 6) to form supercoiled structures, as seen in Fig. 1c (insets). To account for this twist resistance, we defined an empirical equation, based on the following observations (Fig. 2a (inset), Supplementary Fig. 6 and Supplementary Video 3): (1) at $\phi = 0$, we did not expect any resistive torque on the disc from the string; (2) at ϕ_{crit}, the string was at a geomet-
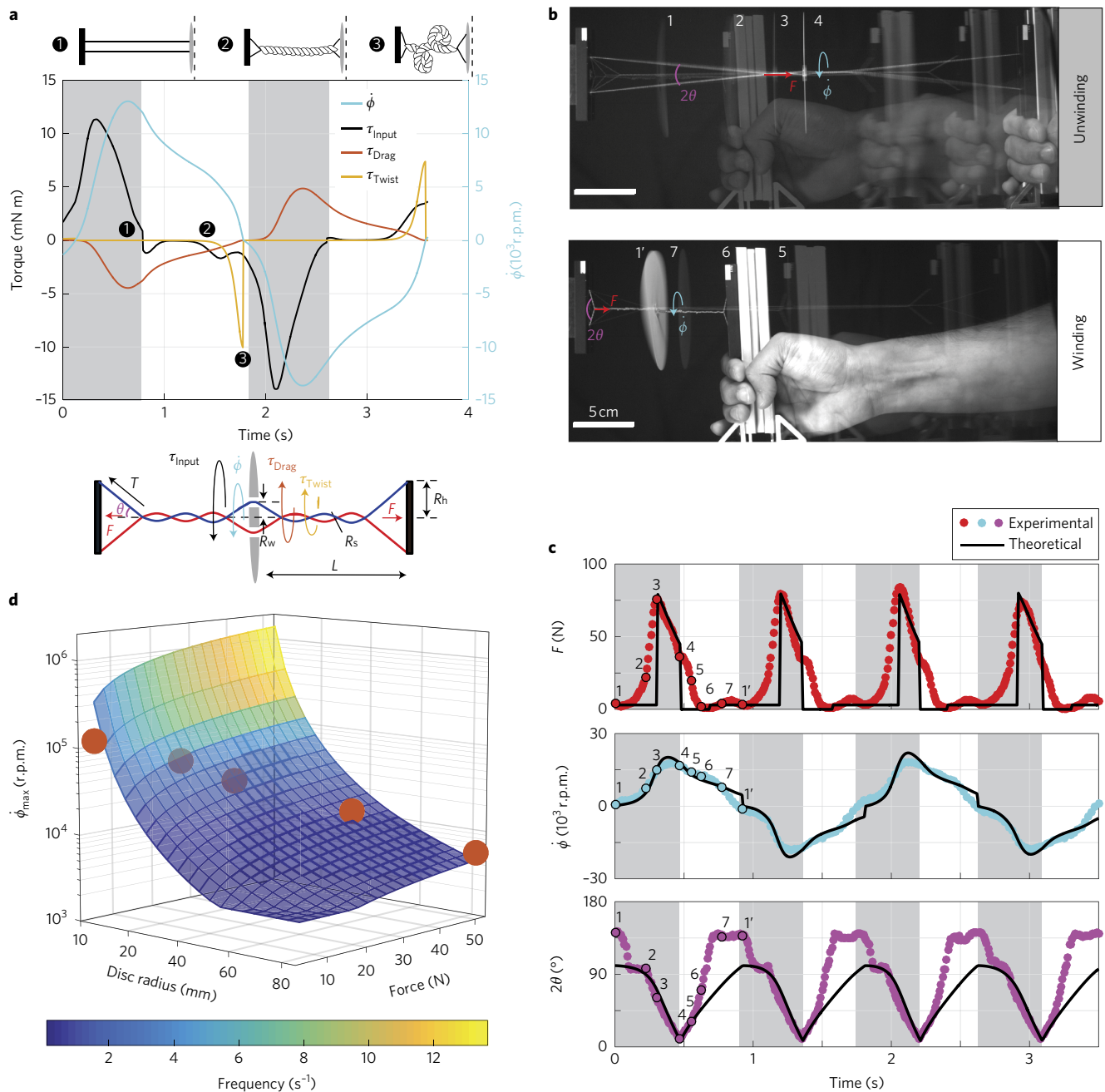
Figure 2 | Validation of the theoretical model with experiments. a, Numerical solution of equation (1) (Supplementary information), highlighting the contributions of different torque components. Schematics illustrate the coiling states (top) and the force−body diagram (bottom) of the paperfuge. **b**, Top: image of four superimposed snapshots (1−4) of the paperfuge during the 'unwinding phase', when F is applied, unwinding the coiled strings and accelerating the paperfuge to its maximum rotational speed (methods in Supplementary Information and Supplementary Video 4). Bottom: four superimposed snapshots (5−1') showing the 'winding phase', when F falls to zero and the inertia of the disc causes re-winding of the strings. **c**, Synchronized time series plots of: force, F (top); $\dot{\phi}$ of the disc (middle); and 2θ of the strings (bottom). The coloured circles denote experimental data and the continuous black lines denote the theoretical predictions, which are in good agreement. When F is approximately zero, low string tension causes the strings to slacken, assuming a geometry outside the scope of our model and causing a systematic underprediction in θ. **d**, The five experimental data points (R_d of 5, 12.5, 25, 50 and 85 mm) along with a set of force-varying data (Supplementary Fig. 5) are used to tune the parameters of our model.

ric critical twist, and further compression was modelled as a linear spring force; and (3) ϕ could not exceed some maximum value ϕ_{max}. Using these conditions, we defined a function of the form:

$$\tau_{Twist}(\phi) = -\,\mathrm{sgn}(\phi)A\left[\frac{1}{(B-|\phi|)^{\gamma}} - C\right] \quad (4)$$

with a twisting parameter (γ), which we fitted using experimental data (Supplementary Fig. 6). The parameters A, B and C were found using the three constraints described above, resulting in the complete expression:

$$\tau_{Twist}(\phi) = -\,\mathrm{sgn}(\phi)\frac{1}{\gamma}(\phi_{max} - \phi_{crit})^{\gamma+1}\left[\frac{1}{(\phi_{max}-|\phi|)^{\gamma}} - \frac{1}{\phi_{max}^{\gamma}}\right] \quad (5)$$
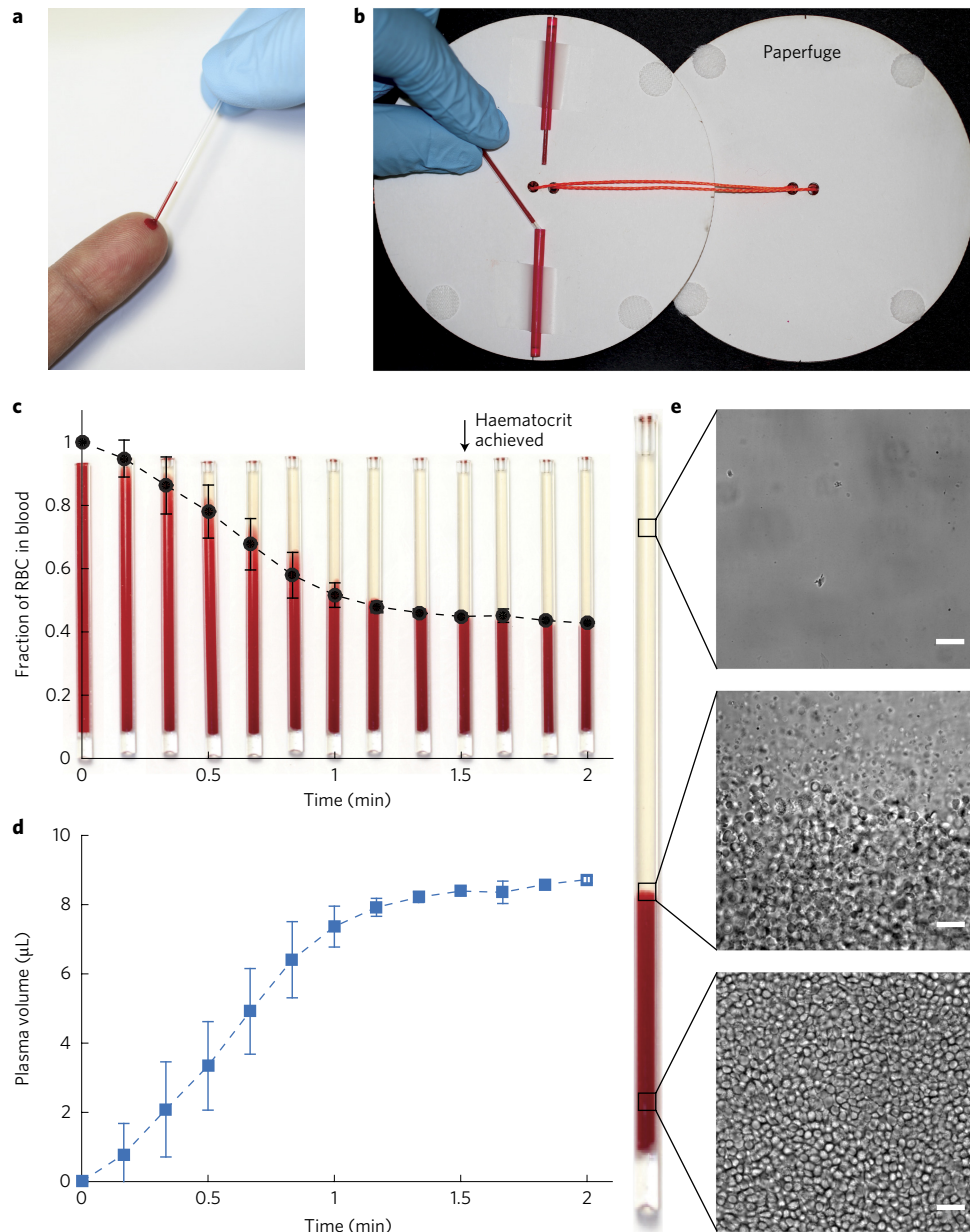
Figure 3 | Paperfuge as a 20-cent diagnostic device for haematocrit analysis. The high rotational speeds of the paperfuge can be exploited in diagnostic sample preparation via centrifugation. **a**, A plastic capillary loaded with 20 μl of human blood. **b**, A capillary placed into hollow plastic capillary holders (with ends sealed) attached to the paperfuge. **c**, Kinetics of red blood cells (RBC) and plasma separation. **d**, Separation of 8 μl of blood plasma (per capillary) from whole blood occurred in less than 1.5 min. Error bars in **c** and **d** represent the standard deviation calculated from eight independent trials conducted by two users (one male, one female), which highlights the consistency and reproducibility of the haematocrit and plasma values. **e**, The quality of the plasma evaluated using microscopy, revealing 100% pure plasma; scale bars are 10 μm.

Knowing the expression for the three torque terms, we numerically solved the differential equation (1) to quantify the dynamics of the buzzer toy (Fig. 2a). Separating the individual contributions of the torque allowed us to see the three stages where each torque term dominated in the cycle. τ_{Input} dominated during the unwinding phase, followed by τ_{Drag}, which reached its maximum value at $\dot{\phi}_{max}$. τ_{Twist} increased drastically at the end of the winding phase $\dot{\phi} = 0$, bringing the disc to a momentary halt, $\dot{\phi} = 0$.

Experimental validation and scaling analysis

By simultaneously measuring applied force and rotational velocity, we quantified the two unknown parameters in our model: a_R and γ. Using a high-speed camera ($f_{rec} = 6,000$ f.p.s.) synchronized with a force transducer, we obtained a time-series of the force actuating the paperfuge (Fig. 2b). By using a simple input function for the force (Supplementary Fig. 7) in our model (equation (1) and Fig. 2c (top)), we accurately predicted the dynamics of the paperfuge (Fig. 2c, middle and bottom). We further utilized the predictive power of our model to develop a design landscape, and compared this with our experimental data (red circles, Fig. 2d). We confirmed the validity of our model for paper discs in the following parameter design space: $R_d = [5, 85]$ mm, $F = [5, 50]$ N, $R_s = [0.05, 0.5]$ mm, $w_d = [0.3, 4.5]$ mm (Supplementary Fig. 11). The scaling curve predicts that 1,000,000 r.p.m. can be achieved at a frequency of oscillation of >10 Hz and nominal forces (50 N). We also highlight the dependence of $\dot{\phi}_{max}$ and f_0 on different
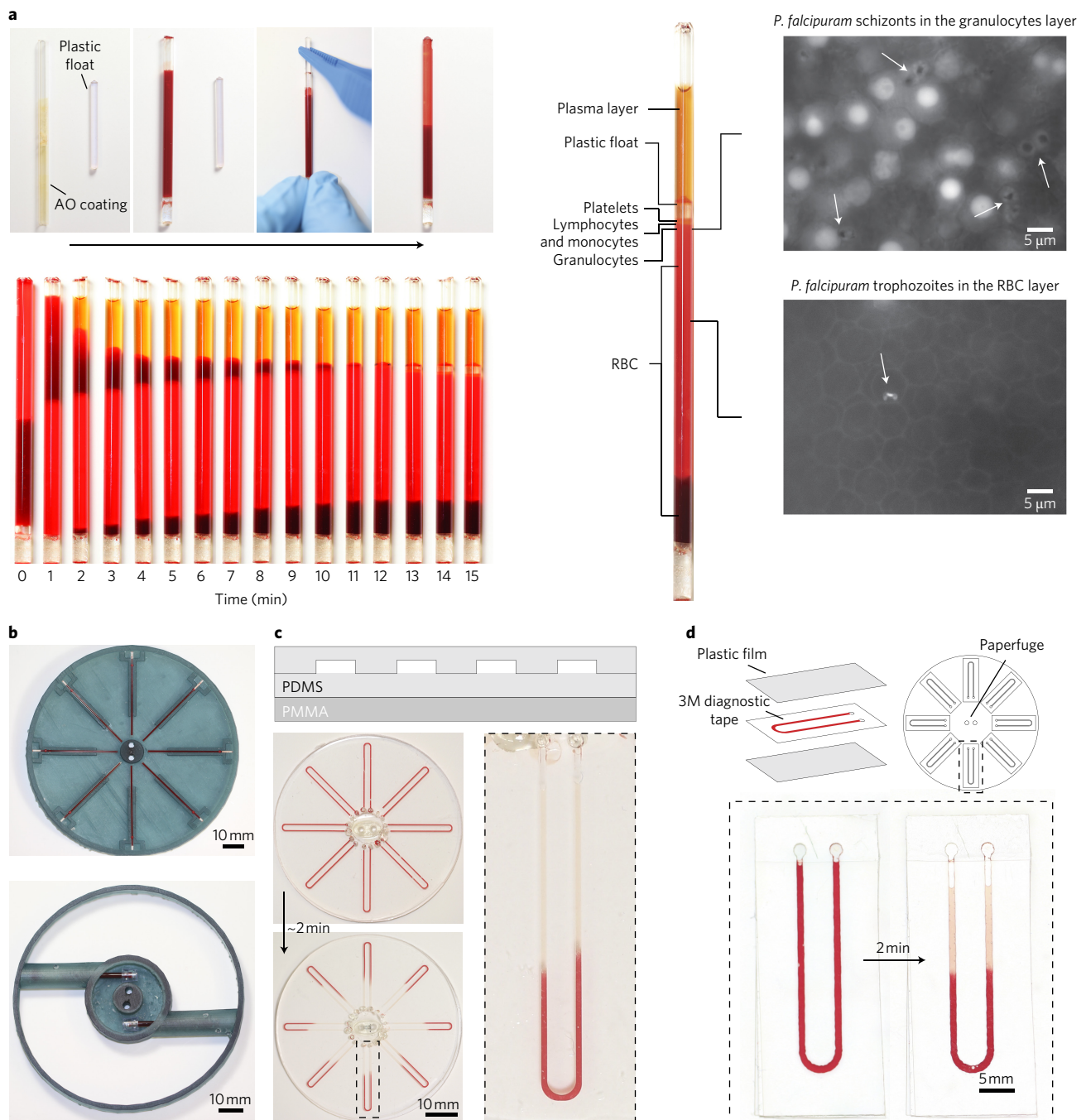
Figure 4 | Paperfuge applications and design landscape. a, QBC for malaria diagnosis. Top four panels: commercial QBC capillary (coated with acridine orange (AO) dye) and solid cylindrical float utilized on the paperfuge to achieve density-based stratification of blood components. Bottom: snapshots of separation over time; at $t=0$, the float is inserted into the top of the capillary; as soon as spinning commences, the float settles to the bottom. Over a period of 15 min, it rises to the plasma/RBC interface due to the difference in density, expanding the buffy-coat region. Right: using *P. falcipuram*-infected blood, the parasite is rapidly visualized using a fluorescent microscope in specific density layers. **b**, 3D-printed devices. Lightweight polymeric materials can be rapidly printed for generating functional low-cost 3D-fuges. The two prototypes shown achieved speeds of approximately 10,000 r.p.m. and weighed <20 g. **c**, Using soft lithography, PDMS devices were fabricated to exploit centrifugal microfluidics. This PDMS-fuge was spun at 15,000 r.p.m., and plasma was separated in 2 min from 10 μl of blood. **d**, Plastic-tape microfluidics. Schematic showing two-dimensional 'slides' constructed using 3M diagnostic tape that can easily be attached to a paperfuge. A two-dimensional slide with a U-shaped channel showed plasma separation from 15 μl whole blood in 2 min.

physical parameters, such as string radius and length, and disc radius and width (Supplementary Fig. 8 and Supplementary Tables 2 and 4).

With our validated model, we optimized the function of the paperfuge for centrifugation. Centrifuges are characterized by the relative centrifugal force (r.c.f.) they can generate, defined as r.c.f. $= R_d \dot{\phi}^2 / g$, where g is the acceleration due to gravity. The paperfuge is an oscillatory centrifuge, which changes direction in a periodic manner. Thus, we defined an effective r.c.f. (Supplementary Fig. 9) as $R_d \langle \dot{\phi}^2(t) \rangle / g$, which yields an r.c.f. $\approx 10,000\,g$ for a paperfuge with $R_d = 50$ mm (see Supplementary Fig. 9 for a table of r.c.f. values for various paperfuge sizes).

Diagnostic applications and design landscape

Next, we demonstrate how the paperfuge can be utilized as a field-portable, ultralow-cost centrifugation tool (Fig. 3a,b, Supplementary Fig. 2 and Supplementary Video 5). We implemented several safety measures to make our device usable in the field (Methods). We filled capillaries with 20 µl of whole human blood (from a finger-prick) and spun them on the paperfuge, revealing complete separation of plasma from the red blood cells (RBC) within 1.5 min (Fig. 3c,d). The volume fraction of RBCs provided a direct readout for hae-matocrit values (packed cell volume, PCV = 0.43, at $t = 1.5$ min), which is a measure used for diagnosing anaemia. The haematocrit value obtained was in good agreement with control experiments conducted simultaneously on a commercial electric centrifuge (Methods). Furthermore, the resulting pure plasma could be easily retrieved for use with other rapid diagnostic tests.

Finally, we show the breadth of possibilities and applications of the paperfuge platform. Using a QBC capillary and float system, we showed that 15 min of spinning on a paperfuge can success-fully separate the buffy coat (Fig. 4a). This expanded region could be easily used for identification of haematoparasites for infectious diseases such as malaria and African trypanosomiasis using a microscope (Fig. 4a and Supplementary Table 1)[16]. A comparison of individual blood components, including platelets, monocytes and granulocytes, revealed good quantitative agreement between the buffy coat obtained with a paperfuge and a commercial electric centrifuge (Supplementary Fig. 10). The simplicity and robustness of the paperfuge device makes it possible to design and construct devices from materials beyond paper, including wood, plastic and polymers. Using a desktop 3D printer (Form 2, Formlabs), we rapidly printed lightweight (20 g) prototypes of different '3D-fuges' that spun at speeds of approximately 10,000 r.p.m. (Fig. 4b). These further open opportunities to mass-manufacture millions of centrifuges using injection-moulding techniques. Moreover, we demonstrated centrifugal microfluidics in a 'PDMS-fuge' (a disc made from polydimethylsiloxane (PDMS), Fig. 4c). This opens up possibilities to design integrated lab-on-a-chip devices that do not require external pumps or electricity[17]. Since soft lithography requires fabrication infrastructure, we showed that inexpensive plastic-tape microfluidics can be used with the paperfuge. We created two-dimensional plastic slides and demonstrated plasma isolation in 2 min, which could be further imaged under a micro-scope without perturbing the sample (Fig. 4d).

Outlook

The in-depth analysis of a simple toy has provided broad inspira-tion for developing human-powered, instrument-free POC devices. The variety of materials (paper, polymers) and rich design land-scape offer potential for electricity-free integrated POC devices. The choice of paper as a substrate further opens opportunities for incorporating origami-based geometries, embedding optics[18], paper-based microfluidics[19] and ultimately integrated lateral-flow rapid diagnostic assays[20]. Moreover, by exploiting the unique oscil-latory dynamics of a paperfuge, new separation protocols could be explored that have been predicted theoretically, but not confirmed empirically[21]. The simplicity of manufacturing our proposed device will enable immediate mass distribution of a solution urgently needed in the field. Ultimately, our present work serves as an exam-ple of frugal science: leveraging the complex physics of a simple toy for global health applications.

Methods

Paperfuge. The paperfuge was composed of two card-stock paper discs (Supplementary Fig. 2a). Braided fishing line (Dyneema, MagicShield) was used for the strings to provide high tensile strength. Common wood or PVC pipe was used for the handles. We used drinking straws to create safe and easy mounting of the capillaries. The straws were sealed using epoxy (J-B Weld 50133, Plastic Bonder) to act as a secondary containment for accidental leakages from the capillaries.

First, two equal circle-shaped discs ($R_d = 50$ mm) were printed on the paper using a laser printer (Epilog Mini Laser). In the centre of each disc, there were two small circular holes (diameter = 3 mm), spaced 2.5 mm apart. During spinning motion, the strings caused extensive friction at the point of contact with the paper. To reduce wear, we used two 3-mm-thick, acrylic ovals (major axis = 13 mm, minor axis = 6 mm) with two small circular holes (diameter = 3 mm), spaced 2.5 mm apart. These acrylic ovals were taped to the centre of the outer face of each disc, such that the holes on the acrylic aligned with the holes on the discs. Two straws were cut down to 40-mm-long pieces. One end of each straw was sealed with a drop of epoxy and allowed to dry for at least 20 min at room temperature. The straws were glued at opposite edges of the inner face of one of the discs, with the epoxy-closed ends pointing outwards. Four Velcro pieces were placed at 90° from each other along the edges of the circular disc. String was threaded through the holes in the centre of the discs and each end of the string was tied around a handle. The two discs were then attached to each other using Velcro, covering the straws (Supplementary Fig. 2b). Sticking the two paper discs together using Velcro serves as a safety cover (see below) as well as creating a streamlined surface for reducing air drag. The paperfuge was spun by holding one handle in each hand (Supplementary Fig. 2c).

User safety measures. The paperfuge included three independent safety mechanisms to protect the user from accidental exposure to blood. First, the capillaries employed were made of shatter-proof plastic. Second, the capillaries were inserted into sealed straw holders that were able to contain accidental leaks. Last, the paperfuge had two discs held together using Velcro strips: one disc held the straw capillary holders and one disc covered the straws. The cover served as an additional safety measure to prevent blood exposure to the user.

Plasma separation from whole human blood. In all the experiments conducted in this study, human blood samples were purchased from Zen-BIO and stored in the fridge at 4 °C until used. Plastic capillaries (40 mm long; SafeCrit microhematocrit heparinized capillary tubes, 22274913, Fisher Scientific) were filled with blood up to the marked line. One end of each capillary was sealed using epoxy and allowed to sit for at least 20 min at room temperature to completely seal the capillary. Each capillary was then mounted into a straw, with the sealed end facing away from the centre.

We conducted more than 50 trials, with two operators (one male, one female). The haematocrit results obtained in 1.5 min on the paperfuge (PCV = 0.43) were comparable to the results obtained using a commercial centrifuge (PCV = 0.47; Critspin, Beckman Coulter) in 2 min. The Critspin centrifuged the blood at a speed of 16,000 r.p.m. (13,700 g) and cost \$700. The paperfuge (with two loaded capillaries) spun at a maximum speed of approximately 20,000 r.p.m. (approximately 10,000 g) and cost 20 cents.

QBC. For QBC analysis using the paperfuge, capillaries coated with acridine orange dye from a QBC malaria test kit (Drucker Diagnostics) were used. The kit also contained a precision plastic float that suspended in the buffy-coat layer post-centrifugation, expanding it for further visualization via brightfield and fluorescent microscopy. To fit on the paperfuge ($R_d = 50$ mm), we cut the QBC capillaries using a diamond cutter. Next, each capillary was filled with 30 µl of blood sample spiked with 7.5% *Plasmodium falcipuram* parasitemia and sealed using epoxy at one end. The float was fully inserted into the open end of each capillary using plastic forceps. Each capillary was then inserted into a straw holder and the paperfuge was spun for 15 min.

Twelve trials of centrifugation were conducted using the QBC capillaries. After the first minute, the float immediately moved to the bottom of the capillary and gradually rose due to its specific density, as the blood separated into plasma and RBCs over 15 min. The buffy coat region was then examined using fluorescent microscopy to identify *P. falcipuram* parasites. Thus, we show proof-of-concept that QBC analysis could be conducted using the paperfuge for infectious diagnostics (Supplementary Table 1). Furthermore, a comparison between the buffy coat obtained using the hand-powered paperfuge and commercial electric centrifuge revealed good quantitative agreement (Supplementary Fig. 10).

PDMS-fuge. The PDMS-fuge was fabricated using the soft lithography technique. First, SU-8 50 resist (MicroChem) was spin-coated on a wafer, followed by prebaking for 10 min, resulting in a 110-µm-thick layer. This was further baked for 30 min to densify the resist film. The resulting resist film was then exposed to ultraviolet light for 18 s, and postbaked for 10 min to selectively crosslink the exposed parts. Finally, the unexposed material was washed away with SU-8 developer to obtain the master mould. To fabricate the channels, a PDMS 20:1 base:curing agent was poured into the mould. A supporting PDMS/PMMA (polymethyl methacrylate)-based structure was also made by pouring a 5:1 base:curing agent mixture onto a circular PMMA disc (1.5 mm thick). Finally, both layers were bonded by incubation at 65 °C overnight. Each U-channel held up to approximately 10 µl of liquid.

Plastic-tape microfluidics. Plastic-tape microfluidics provided an easy to use, low-cost, disposable platform for centrifuging biological samples. The slides were assembled using double-sided tape (3M 9965 double-coated polyester diagnostic tape) and thin plastic films (3M pp2500 transparency film). First, U-shaped channels were laser-printed onto two sheets of double-sided tape. Each side of the tape was then adhered to a thin plastic film and the entire microfluidic channel was clamped for 15 min to seal the sides of the channel. A drop of blood (approximately 10 μl) was applied to the top of the channel and capillary action drew the blood into the channel in a few seconds. These slides were then mounted on a paperfuge and spun normally. Alternatively, paper could be used as the channel layer, and single-sided tape could be used to seal from both sides.

High-speed dynamics setup. To measure the dynamic force, we used an S-type load cell (CZL301C, Phidgets). The load cell was connected to an Arduino (RedBoard, SparkFun Electronics) using a load-amplifying circuit board (HX711, SparkFun Elec). Custom code was written to calibrate the load cell with known weights and measure the force output when connected to one end of the paperfuge setup. High-speed videos were recorded using two high-speed cameras. Analysis was done using custom script written in Matlab.

Code availability. The source code for the mathematical model of the mechanics of the paperfuge can be accessed at the Zenodo Repository (http://dx.doi.org/10.5281/zenodo.166336).

Data availability. The authors declare that all data supporting the findings of this study are available within the paper and its Supplementary Information.

References

1. Mabey, D., Peeling, R. W., Ustianowski, A. & Perkins, M. D. Tropical infectious diseases: diagnostics for the developing world. *Nat. Rev. Microbiol.* **2**, 231–240 (2004).
2. Al-Soud, W. A. & Rådström, P. Purification and characterization of PCR-inhibitory components in blood cells. *J. Clin. Microbiol.* **39**, 485–493 (2001).
3. Singleton, J. *et al.* Electricity-free amplification and detection for molecular point-of-care diagnosis of HIV-1. *PLoS ONE* **9**, e113693 (2014).
4. LaBarre, P., Boyle, D., Hawkins, K. & Weigl, B. Instrument-free nucleic acid amplification assays for global health settings. *Proc. SPIE* **8029**, 802902 (2011).
5. Niemz, A., Ferguson, T. M. & Boyle, D. S. Point-of-care nucleic acid testing for infectious diseases. *Trends Biotechnol.* **29**, 240–250 (2011).
6. Brown, J. *et al.* A hand-powered, portable, low-cost centrifuge for diagnosing anemia in low-resource settings. *Am. J. Trop. Med. Hyg.* **85**, 327–332 (2011).
7. Wong, A. P., Gupta, M., Shevkoplyas, S. S. & Whitesides, G. M. Egg beater as centrifuge: isolating human blood plasma from whole blood in resource-poor settings. *Lab Chip* **8**, 2032–2037 (2008).
8. Mariella, R. Jr Sample preparation: the weak link in microfluidics-based biodetection. *Biomed. Microdevices* **10**, 777–784 (2008).
9. Dineva, M. A., Mahilum-Tapay, L. & Lee, H. Sample preparation: a challenge in the development of point-of-care nucleic acid-based assays for resource-limited settings. *Analyst* **132**, 1193–1199 (2007).
10. Urdea, M. *et al.* Requirements for high impact diagnostics in the developing world. *Nature* **444**, 73–79 (2006).
11. Bohr, J. & Olsen, K. The ancient art of laying rope. *Europhys. Lett.* **93**, 60004 (2011).
12. van der Heijden, G. H. M. & Thompson, J. M. T. Helical and localised buckling in twisted rods: a unified analysis of the symmetric case. *Nonlinear Dynam.* **21**, 71 (2000).
13. Ricca, R. L. The energy spectrum of a twisted flexible string under elastic relaxation. *J. Phys. A: Math. Gen.* **28**, 2335–2352 (1995).
14. Freund, H. J. Time control of hand movements. *Prog. Brain Res.* **64**, 287–294 (1986).
15. Schlichting, H. J. & Suhr, W. The buzzer—a novel physical perspective on a classical toy. *Eur. J. Phys.* **31**, 501–510 (2010).
16. Adeoye, G. O. & Nga, I. C. Comparison of quantitative buffy coat technique (QBC) with giemsa-stained thick film (GTF) for diagnosis of malaria. *Parasitol. Int.* **56**, 308–312 (2007).
17. Gorkin, R. *et al.* Centrifugal microfluidics for biomedical applications. *Lab Chip* **10**, 1758–1773 (2010).
18. Cybulski, J. S., Clements, J. & Prakash, M. Foldscope: origami-based paper microscope. *PLoS ONE* **9**, e98781 (2014).
19. Martinez, A. W., Phillips, S. T., Whitesides, G. M. & Carrilho, E. Diagnostics for the developing world: microfluidic paper-based analytical devices. *Anal. Chem.* **82**, 3–10 (2010).
20. Yager, P. *et al.* Microfluidic diagnostic technologies for global public health. *Nature* **442**, 412–418 (2006).
21. Xu, S. & Nadim, A. Oscillatory counter-centrifugation. *Phys. Fluids* **28**, 021302 (2016).

Acknowledgements

Author contributions

M.S.B. and M.P. designed the research; M.S.B., B.B., C.C., G.K. and A.J. performed and analysed the research; all authors wrote the paper.

Additional information

Supplementary information is available for this paper.

Reprints and permissions information is available at www.nature.com/reprints.

Correspondence and requests for materials should be addressed to P.M.

How to cite this article: Bhamla, M. S. *et al.* Hand-powered ultralow-cost paper centrifuge. *Nat. Biomed. Eng.* **1**, 0009 (2017).

Competing interests

The authors declare no competing financial interests.